Original Article

Ultrasound elastography features as promising predictors of pathological complete response in patients with HER2-positive breast cancer undergoing neoadjuvant therapy

Wei Xiang1*, Xiaohui Sun2*, Yiru Cheng1, Jianli Xue1

¹Department of Ultrasound, The Fourth Hospital of Shijiazhuang, Shijiazhuang 050000, Hebei, China; ²Prenatal Diagnosis Sub-Center, The Fourth Hospital of Shijiazhuang, Shijiazhuang 050000, Hebei, China. *Co-first authors.

Received July 11, 2025; Accepted September 15, 2025; Epub October 15, 2025; Published October 30, 2025

Abstract: Objectives: Human epidermal growth factor receptor 2 (HER2)-positive breast cancer is an aggressive subtype; however, neoadjuvant therapy (NAT) can improve patient outcomes. Accurate prediction of pathological complete response (pCR) is crucial for guiding treatment adjustments. This study aimed to evaluate the predictive value of ultrasound elastography features for pCR in patients with HER2-positive breast cancer undergoing NAT. Methods: This retrospective study included 80 patients with HER2-positive breast cancer who received NAT and were evaluated for pCR by histopathological examination. Ultrasound elastography features, including strain ratio and strain difference, were compared between patients achieving pCR (n = 36) and those without pCR (n = 44). Logistic regression and receiver operating characteristic curve analyses were performed. An external validation cohort of 72 patients was used to assess model robustness. Results: Posterior shadowing on ultrasound and lower strain ratio and difference at six weeks were significantly associated with higher pCR rates. Logistic regression identified posterior shadowing (OR = 6.634, P = 0.008), strain ratio (OR = 0.064, P = 0.022), and strain difference (OR = 0.678, P < 0.001) as independent predictors of pCR. The combined predictive model demonstrated excellent performance, with an area under the curve of 0.871 in the primary cohort and 0.884 in the validation cohort. Conclusion: Ultrasound elastography features, particularly posterior shadowing and changes in strain metrics, are independent predictors of pCR in patients with HER2-positive breast cancer receiving NAT.

Keywords: HER2-positive breast cancer, neoadjuvant therapy, pathological complete response, ultrasound elastography, shear wave elastography, predictive biomarkers

Introduction

Breast cancer remains a major global health challenge, with approximately 15-20% of cases classified as human epidermal growth factor receptor 2 (HER2)-positive. HER2-positive breast cancer is characterized by an aggressive clinical course; however, the advent of targeted therapies has significantly improved the prognosis of this subgroup [1, 2]. Neoadjuvant therapy (NAT) plays a pivotal role in managing HER2-positive breast cancer by reducing tumor burden, thereby enhancing surgical outcomes and providing an early indication of therapeutic efficacy. Achieving a pathological complete response (pCR) after NAT is strongly associated

with improved long-term outcomes, including disease-free survival and overall survival [3, 4].

In recent years, predicting pCR has attracted increasing attention because of its potential to individualize treatment strategies and improve patient outcomes. Although traditional imaging modalities are valuable, they often fall short in the early prediction of therapeutic response. This limitation highlights the need for novel diagnostic approaches that can provide reliable and timely indicators of treatment effectiveness. Advances in ultrasound (US) technology, particularly elastography, offer a promising avenue to enhance the predictive accuracy of response assessment in breast cancer management [5, 6].

US elastography, a noninvasive imaging technique, enables real-time assessment of tissue elasticity. It is based on the principle that malignant tissues are typically stiffer than their benign or normal counterparts. Elastography provides quantitative measures such as strain ratio and strain difference, which were indicative of tissue stiffness and can reflect early biological changes in tumors responding to NAT. The integration of shear-wave elastography with conventional sonography has further expanded the diagnostic capabilities of US, offering additional data that may help determine pathological status after treatment [7-9].

Recent studies have investigated the utility of US elastography in distinguishing malignant from benign breast lesions. However, its specific application in predicting pCR in patients with HER2-positive breast cancer undergoing NAT remains insufficiently explored. Identifying elastographic features that correlate with pCR could serve as a valuable tool for tailoring treatment strategies [10, 11].

Despite its potential, challenges remain in the standardized application and interpretation of US elastography. Variability in measurement techniques, operator dependency, and limited understanding of the biological mechanisms linking elastographic changes to histopathological outcomes continue to pose significant obstacles [12, 13].

This study aims to address this gap by evaluating the predictive value of US elastographyderived features for assessing pCR in patients with HER2-positive breast cancer undergoing NAT.

Materials and methods

Ethics statement

This study was approved by the Institutional Review Board and Ethics Committee of The Fourth Hospital of Shijiazhuang. As a retrospective analysis using only de-identified patient data, the requirement for informed consent was waived. The waiver was granted because the study posed no risk of harm or impact on patient care and was conducted in accordance with applicable regulatory and ethical guidelines for retrospective research.

Study design

This study included 80 patients with HER2positive breast cancer who received NAT at The Fourth Hospital of Shijiazhuang between 2023 and 2024. The objective was to evaluate the predictive value of US elastography-derived features for determining pCR by reviewing patient medical records. Histopathological examination was used to classify patients into a pCR group (n = 36) and a non-pCR group (n = 44). For external validation, an additional cohort of 72 patients with HER2-positive breast cancer from the same institution was analyzed using identical inclusion criteria and grouping methods. This validation cohort comprised 31 patients in the pCR group and 41 patients in the non-pCR group.

Eligibility and grouping criteria

The inclusion criteria were as follows: female patients with unilateral breast cancer, aged 18 years or older, newly diagnosed according to the World Health Organization classification guidelines for breast cancer [14]. Eligible patients were required to have confirmed HER2-positive status and have undergone surgery after NAT. Before initiation of chemotherapy, all participants had to undergo both conventional US and shear-wave elastography, as well as core needle biopsy for histopathological confirmation. In addition, pathological specimens had to be well preserved, and complete clinical and pathological data were required.

The exclusion criteria were as follows: patients with inflammatory breast cancer; a prior history of breast abnormalities, major trauma, or breast surgery; or skin abnormalities. Patients with a current or past history of connective tissue disease, pregnancy, or lactation were also excluded. In addition, patients with a history of local radiotherapy or systemic chemotherapy, or breast lesions larger than 8 cm in diameter, were deemed ineligible. Patients with acute diseases (e.g., infection or fever), those unsuitable for US examination, individuals with obesity (body mass index [BMI] > 30), mental disorders, or metallic implants such as cardiac pacemakers were likewise excluded.

Patients were categorized according to the Response Evaluation Criteria in Solid Tumors.

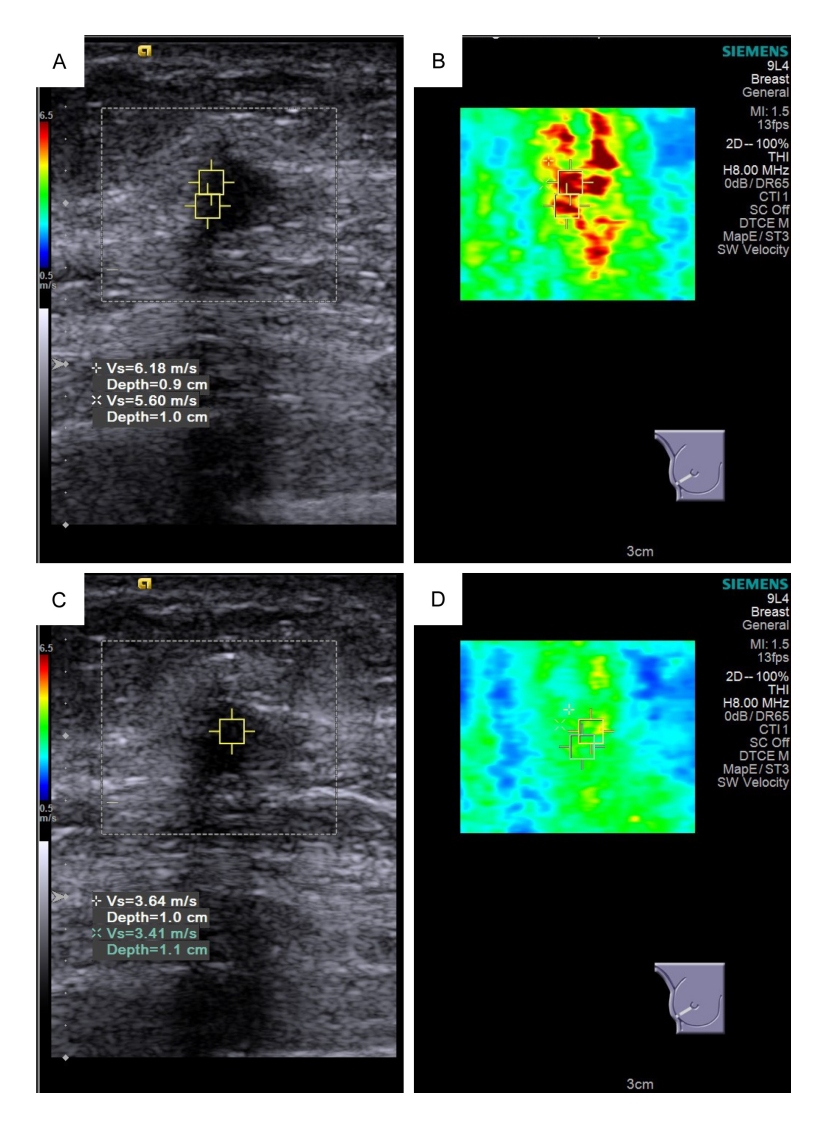


Figure 1. Breast ultrasound and elastography. A. Ultrasound image of a breast lesion before treatment; B. Elastography image of the breast before treatment; C. Ultrasound image of a breast lesion after treatment; D. Elastography image of the breast after treatment.

Those with no residual invasive cancer cells in surgically resected primary tumor specimens, as confirmed by microscopic examination, were classified into the pCR group [15]. Patients with residual tumor cells identified during post-operative pathological examination were classified into the non-pCR group. The quantity and distribution of residual tumor cells were considered in guiding subsequent treatment decisions. To ensure consistency and accuracy, all pathology slides were reviewed by an independent pathologist. The same grouping criteria were applied to the external validation cohort.

Ultrasonography

Ultrasound examinations were performed using the Siemens ACUSON Sequoia color Doppler system equipped with a PTL-1005BT linear array probe and software for elastic imaging and strain rate measurement. Patients underwent imaging both before initiation of neoadjuvant chemotherapy (NAC) and at the sixth week of treatment. All examinations were conducted with patients in the supine position to ensure complete exposure of the breasts. Each quadrant of the affected breast was systematically scanned (Figure 1). Once the lesion was identified, multi-sectional US scanning was performed to evaluate tumor size, aspect ratio, margins, internal echoes, posterior features, posterior echoes, architectural distortion, and abnormal vascularity. All findings were interpreted according to the American College of Radiology Breast Imaging Reporting and Data System UItrasound, Fifth Edition [16]. Under elastography mode, light vertical compression and decompression were applied at a frequency of 2-3 times per second. The sampling frame included both the lesion and

adjacent tissue. After generating the strain map, regions corresponding to the lesion and surrounding tissue at equivalent levels were selected to calculate the strain ratio and strain difference. The strain ratio was obtained by dividing the strain value of the lesion area by that of the adjacent normal tissue, whereas the strain difference was calculated by subtracting the normal tissue strain value from that of the lesion.

Pathological examination

Pathological examination was performed after surgical resection of the lesions. The tissue

Table 1. Comparison of demographic and baseline characteristics

Parameters	Non-pCR Group (n = 44)	pCR Group (n = 36)	t/χ²	Р
Age (years)	51.97 ± 7.62	52.39 ± 6.78	0.260	0.796
BMI (kg/m ²)	21.16 ± 2.17	21.36 ± 2.34	0.386	0.701
Marital status (married/others)	40 (90.91%)/4 (9.09%)	31 (86.11%)/5 (13.89%)	0.102	0.749
Family history of breast cancer	8 (18.18%)	6 (16.67%)	0.031	0.859
History of malignancy	7 (15.91%)	5 (13.89%)	0.063	0.801
Menopause status			3.791	0.150
Premenopausal	24 (54.55%)	12 (33.33%)		
Postmenopausa	19 (43.18%)	22 (61.11%)		
Perimenopasual	1 (2.27%)	2 (5.56%)		
NAC regimen			0.208	0.976
Doxorubicin, Cyclophosphamide, and Paclitaxel	22 (50.00%)	19 (52.78%)		
5-Fluorouracil, Epirubicin, Cyclophosphamide, and Docetaxel	16 (36.36%)	13 (36.11%)		
Docetaxel and Cyclophosphamide	4 (9.09%)	3 (8.33%)		
Adriamycin, Cyclophosphamide, and Docetaxel	2 (4.55%)	1 (2.78%)		
Lymphedema	11 (25.00%)	8 (22.22%)	0.084	0.771
Arrhythmia	3 (6.82%)	1 (2.78%)	0.096	0.757
Cognitive dysfunction	12 (27.27%)	9 (25.00%)	0.053	0.818
Hand-foot syndrome	15 (34.09%)	12 (33.33%)	0.005	0.943

pCR: pathological complete response; BMI: body mass index; NAC: neoadjuvant chemotherapy.

samples were processed through fixation in 10% formalin, dehydration, immersion, paraffin embedding, serial sectioning, and sealing for histopathological evaluation. Two pathologists independently diagnosed and documented the lesions in accordance with the kit instructions (EY-01H306, Yiyan Biotechnology Co., Ltd., Shanghai, China). Assessment of pCR was based on the Response Evaluation Criteria in Solid Tumors [17]. This evaluation included precise measurement of tumor size, microscopic determination of tumor type by assessing tissue morphology, and identification of molecular features through immunohistochemical analysis of estrogen receptor, progesterone receptor, HER2, and hormone receptor expression.

Statistical analysis

Data analyses were performed using SPSS version 29.0 (SPSS Inc., Chicago, IL, USA). The Shapiro-Wilk test was applied to assess the normality of continuous variables. Normally distributed data were presented as mean ± standard deviation, whereas non-normally distributed data were expressed as median with interquartile range. Categorical variables were summarized as frequencies and percentages [n (%)]. Independent-samples t-tests and Mann-

Whitney U tests were used for normally and non-normally distributed variables, respectively. Chi-square tests or Fisher's exact tests were employed for categorical variables.

Univariate correlation analyses were performed to explore associations between US features and pCR. Variables with P < 0.1 in univariate analysis were entered into multivariate logistic regression models, which applied stepwise backward elimination to retain predictors significant at P < 0.05. Receiver operating characteristic (ROC) curves were plotted to evaluate diagnostic performance, and the area under the curve (AUC) were calculated. Optimal cutoff values, sensitivity, specificity, and likelihood ratios were determined. Model stability and generalizability were further assessed using the external validation cohort.

Results

Demographic and baseline characteristics

A total of 80 patients were included, comprising 36 patients in the pCR group and 44 in the non-pCR group (**Table 1**). The mean age did not differ significantly between the two groups (P = 0.796). BMI was also comparable (P = 0.701).

Table 2. Comparison of pathological characteristics

Parameters	Non-pCR Group ($n = 44$)	pCR Group ($n = 36$)	t/χ^2	Р
Initial tumor size (cm)	5.15 ± 1.94	5.24 ± 2.01	0.198	0.844
Tumor grade			0.324	0.850
I	2 (4.55%)	2 (5.56%)		
II	16 (36.36%)	15 (41.67%)		
III	26 (59.09%)	19 (52.78%)		
Histology			0.043	0.979
Invasive ductal carcinoma	37 (84.09%)	30 (83.33%)		
Invasive lobular carcinoma	2 (4.55%)	2 (5.56%)		
Invasive metaplastic carcinoma	5 (11.36%)	4 (11.11%)		
Molecular features			1.719	0.423
ER+ & PR+ & HER2+	25 (56.82%)	18 (50.00%)		
ER+ & PR- & HER2+	8 (18.18%)	11 (30.56%)		
ER- & PR- & HER2+	11 (25.00%)	7 (19.44%)		
Hormone receptor			0.241	0.624
Positive	17 (38.64%)	12 (33.33%)		
Negative	27 (61.36%)	24 (66.67%)		

pCR: pathological complete response; ER+: estrogen receptor-positive; PR+: progesterone receptor-positive; HER2+: human epidermal growth factor receptor 2-positive.

Marital status, family history of breast cancer, and prior history of malignancy showed no significant differences between groups (P > 0.740 for all). Menopause status was not significantly different (P = 0.150). The distribution of NAT regimens were similar across groups (P = 0.976). In addition, no significant differences were observed in the incidence of lymphedema (P = 0.771), arrhythmia (P = 0.757), cognitive dysfunction (P = 0.818), or hand-foot syndrome (P = 0.943). These findings indicate that demographic and clinical characteristics were well balanced between groups, thereby providing a reliable basis for subsequent analyses of US elastography features.

Pathological characteristics

Initial tumor size was comparable between the pCR and non-pCR groups (P = 0.844) (**Table 2**). Tumor grade distribution also showed no significant differences, with grade III tumors predominating in both groups (P = 0.850). The predominant histological type was invasive ductal carcinoma in both groups (P = 0.979). Molecular feature analysis revealed no significant differences, with similar distributions of estrogen receptor-positive, progesterone receptor-positive, and HER-positive tumors (P = 0.423). Hormone receptor status was likewise consis-

tent between groups (P = 0.624). These comparable pathological characteristics provide a solid foundation for subsequent evaluation of the predictive value of US elastography features.

US characteristics

The pCR group exhibited a significantly higher incidence of posterior shadowing compared to the non-pCR group (P = 0.002) (Table 3). No statistically significant differences were observed for other parameters. Tumor size (P = 0.098) and margins characterized by spiculations (P = 0.11) were similar between the groups. The tumor aspect ratio was predominantly ≤ 1 in both groups (P = 0.5), and internal echo patterns were mostly uneven (P = 0.41). Tumor posterior echo and calcification did not show significant differences (P = 0.172 and P = 0.058, respectively). Distortion and abnormal blood flow signals were also comparable between the groups (P = 0.769 and P = 0.927, respectively). These findings indicate that among several US features, only posterior shadowing was significantly associated with pCR at six weeks.

At baseline, there were no significant differences in the strain ratio and strain difference

Table 3. Comparison of US characteristics at six weeks

Parameters	Non-pCR Group (n = 44)	pCR Group (n = 36)	t/χ²	Р
Size (mm)	3.15 ± 1.01	2.76 ± 1.02	1.676	0.098
Tumor aspect ratio			0.455	0.500
≤ 1	41 (93.18%)	31 (86.11%)		
> 1	3 (6.82%)	5 (13.89%)		
Margins			2.548	0.110
Spiculations	25 (56.82%)	14 (38.89%)		
No spiculations	19 (43.18%)	22 (61.11%)		
Tumor internal echo			0.679	0.410
Uniform	6 (13.64%)	2 (5.56%)		
Uneven	38 (86.36%)	34 (94.44%)		
Posterior features			9.426	0.002
Shadowing	6 (13.64%)	16 (44.44%)		
No shadowing	38 (86.36%)	20 (55.56%)		
Tumor posterior echo			3.515	0.172
Attenuation	14 (31.82%)	5 (13.89%)		
Unchanged	29 (65.91%)	30 (83.33%)		
Enhancement	1 (2.27%)	1 (2.78%)		
Calcifications			3.585	0.058
Absent	24 (54.55%)	27 (75.00%)		
Present	20 (45.45%)	9 (25.00%)		
Distortion			0.086	0.769
Absent	7 (15.91%)	4 (11.11%)		
Present	37 (84.09%)	32 (88.89%)		
Abnormal blood flow signal			0.008	0.927
Positive	7 (15.91%)	6 (16.67%)		
Negative	37 (84.09%)	30 (83.33%)		

pCR: pathological complete response; US: ultrasound.

between the non-pCR and pCR groups. By week 6, the pCR group showed significantly lower strain ratio and strain difference compared to the non-pCR group (P < 0.01 and P < 0.001, respectively) (**Figure 2**). These results suggest that changes in strain measurements at week 6 may serve as predictors of pCR.

Correlation analysis

Posterior features, including shadowing or its absence, showed a moderate positive correlation with pCR, which was statistically significant (P = 0.002) (**Table 4**). A negative correlation was observed with the strain ratio at week 6 (P = 0.003), indicating that lower strain ratios were associated with a higher likelihood of achieving pCR. Additionally, the strain difference at week 6 demonstrated a stronger negative correlation, with a highly significant P Value

(P < 0.001), underscoring its potential as a predictive marker. These findings suggest that specific US elastography features, particularly posterior features and strain differences, may serve as useful predictors of pCR in this patient cohort.

Logistic regression analysis

The presence of posterior shadowing significantly increased the likelihood of achieving pCR (P = 0.003) (**Table 5**). The strain ratio at week 6 was negatively associated with pCR (P = 0.007), indicating that higher strain ratios were associated with lower probabilities of pCR. Additionally, the strain difference at week 6 also showed a significantly negative correlation with pCR (P < 0.001), highlighting its potential as a predictive marker. These findings suggest that specific US elastography features,

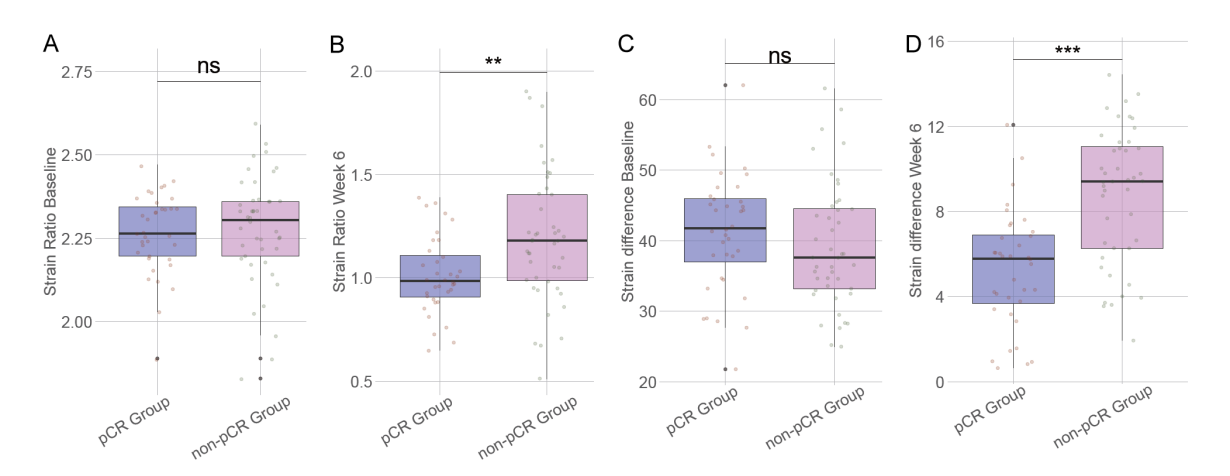


Figure 2. Comparison of strain ratio and strain difference. A. Strain ratio at baseline; B. Strain ratio at week 6; C. Strain difference at baseline; D. Strain difference at week 6. pCR: pathological complete response; ns: no statistically significant difference; **: P < 0.01; ***: P < 0.001.

Table 4. Correlation analysis of US features based on elastography for predicting pCR in HER2-positive breast cancer patients undergoing NAT

Influencing factors	rho	Р
Posterior features (shadowing/no shadowing)	0.343	0.002
Strain ratio at week 6	-0.330	0.003
Strain difference at week 6	-0.498	< 0.001

US: ultrasound; pCR: pathological complete response; NAT: neoadjuvant therapy; HER2: human epidermal growth factor receptor 2.

undergoing NAT, we integrated predictive variables including posterior features, strain ratio at week 6, and strain difference at week 6 (**Figure 3**). The model demonstrated an AUC of 0.871, reflecting a high degree of predictive accuracy for pCR in this patient cohort.

particularly posterior shadowing and strain differences, play a key role in predicting pCR in this patient cohort.

In the multivariate logistic regression analysis evaluating US elastography features for predicting pCR in HER2-positive breast cancer patients undergoing NAT, independent risk factors were identified (Table 6). Posterior shadowing significantly increased the likelihood of pCR (P = 0.008). The strain ratio at week 6 was inversely associated with pCR (P = 0.022), suggesting that higher strain ratios predicted lower odds of pCR. Furthermore, the strain difference at week 6 was negatively correlated with pCR outcomes (P < 0.001), indicating its relevance as a predictive marker. These results underscore the potential of specific US elastography features, especially posterior shadowing and strain differences, as effective predictors of pCR in this patient population.

ROC curve

To construct a combined predictive model for pCR in HER2-positive breast cancer patients

External validation of the predictive model

In the external validation cohort evaluating the predictive value of US elastography features. the mean age was comparable between the non-pCR and pCR groups (P = 0.797) (**Table 7**). BMI also showed no significant difference (P = 0.588). Marital status and family history of breast cancer were similar between the groups. with P Values of 0.943 and 0.915, respectively. The distribution of menopausal status and NAC regimens did not significantly differ (P = 0.222 and P = 0.989, respectively). Additionally, no significant differences were observed in the prevalence of lymphedema, arrhythmia, cognitive dysfunction, or hand-foot syndrome, with P Values of 0.858, 0.817, 0.785, and 0.537, respectively. These results indicate that the groups were largely similar in terms of these baseline characteristics, supporting the robustness of the subsequent analysis of US elastography features.

Compared to the non-pCR group, posterior shadowing was observed more frequently in

Table 5. Univariate logistic regression analysis of US features based on elastography for predicting pCR in HER2-positive breast cancer patients undergoing NAT

Influencing factors	Coefficient	Std error	Wald	Р	OR	95% CI
Posterior features (shadowing/no shadowing)	1.623	0.553	2.936	0.003	5.067	1.788-16.038
Strain ratio at week 6	-2.756	1.017	2.710	0.007	0.064	0.007-0.406
Strain difference at week 6	-0.376	0.093	4.054	< 0.001	0.687	0.562-0.812

US: ultrasound; pCR: pathological complete response; NAT: neoadjuvant therapy; HER2: human epidermal growth factor receptor 2; CI: confidence interval; Std: standard deviation; OR: odds ratio.

Table 6. Multivariate logistic regression analysis of US features based on elastography for predicting pCR in HER2-positive breast cancer patients undergoing NAT

Influencing factors	Coefficient	Std error	Wald	Р	OR	95% CI lower	95% CI upper
Posterior features (shadowing/no shadowing, shadowing:1)	1.892	0.711	2.661	0.008	6.634	1.646	26.737
Strain ratio at week 6	-2.756	1.205	-2.288	0.022	0.064	0.006	0.674
Strain difference at week 6	-0.389	0.106	-3.657	< 0.001	0.678	0.550	0.835

US: ultrasound; pCR: pathological complete response; NAT: neoadjuvant therapy; HER2: human epidermal growth factor receptor 2; CI: confidence interval; Std: standard deviation; OR: odds ratio.

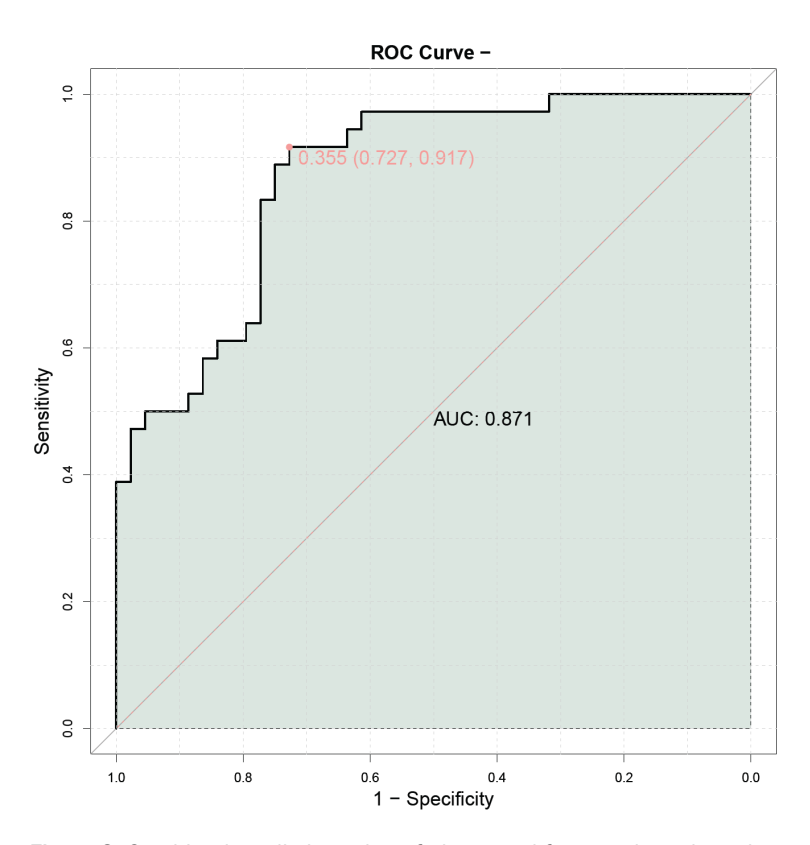


Figure 3. Combined predictive value of ultrasound features based on elastography for predicting pCR in HER2-positive breast cancer patients undergoing NAT. ROC: receiver operating characteristic; AUC: area under the curve; HER2: human epidermal growth factor receptor 2; pCR: pathological complete response; NAT: neoadjuvant therapy.

the pCR group (P = 0.004) (Table 8). The strain ratio at baseline was similar between the

groups (P = 0.884); however. at week 6, the pCR group showed a significantly lower strain ratio compared to the non-pCR group, indicating a marked reduction in stiffness in responders (P = 0.001). Similarly, the baseline strain difference did not significantly differ between the groups (P = 0.254), but by week 6, the pCR group exhibited a significantly greater reduction in strain difference compared to the nonpCR group (P < 0.001). These findings underscore the utility of specific US elastography features in predicting pCR in HER2-positive breast cancer patients receiving NAT.

ROC (external validation)

In the external validation cohort, we constructed a combined predictive model for pCR in HER2-positive breast cancer patients undergoing NAT integrating predictive variables, including posterior features, strain ratio at week 6, and

strain difference at week 6 (Figure 4). This model demonstrated an AUC of 0.884, reflect-

Table 7. Basic characteristics for external validation

Parameters	Non-pCR Group $(n = 41)$	pCR Group (n = 31)	t/χ²	Р
Age (years)	52.39 ± 6.75	51.99 ± 6.18	0.258	0.797
BMI (kg/m²)	21.43 ± 2.09	21.72 ± 2.27	0.544	0.588
Marital status (married/others)	37 (90.24%)/4 (9.76%)	29 (93.55%)/2 (6.45%)	0.005	0.943
Family history of breast cancer	7 (17.07%)	5 (16.13%)	0.011	0.915
History of malignancy	5 (12.20%)	2 (6.45%)	0.170	0.680
Menopause status			3.011	0.222
Premenopausal	21 (51.22%)	10 (32.26%)		
Postmenopausa	18 (43.90%)	20 (64.52%)		
Perimenopasual	2 (4.88%)	1 (3.23%)		
NAC regimen			0.125	0.989
Doxorubicin, Cyclophosphamide, and Paclitaxel	21 (51.22%)	16 (51.61%)		
5-Fluorouracil, Epirubicin, Cyclophosphamide, and Docetaxel	14 (34.15%)	11 (35.48%)		
Docetaxel and Cyclophosphamide	4 (9.76%)	3 (9.68%)		
Adriamycin, Cyclophosphamide, and Docetaxel	2 (4.88%)	1 (3.23%)		
Lymphedema	10 (24.39%)	7 (22.58%)	0.032	0.858
Arrhythmia	3 (7.32%)	1 (3.23%)	0.053	0.817
Cognitive dysfunction	12 (29.27%)	10 (32.26%)	0.074	0.785
Hand-foot syndrome	13 (31.71%)	12 (38.71%)	0.382	0.537

pCR: pathological complete response; BMI: body mass index; NAC: neoadjuvant chemotherapy.

Table 8. Comparison of parameters for external validation

Parameters	Non-pCR Group (n = 41)	pCR Group (n = 31)	t/χ²	Р
Posterior features			8.158	0.004
Shadowing	7 (17.07%)	15 (48.39%)		
No shadowing	34 (82.93%)	16 (51.61%)		
Strain ratio				
Baseline	2.15 ± 0.32	2.16 ± 0.15	0.146	0.884
Week 6	1.18 ± 0.21	0.99 ± 0.27	3.393	0.001
Strain difference				
Baseline (%)	32.18 ± 5.74	33.85 ± 6.54	1.150	0.254
Week 6 (%)	9.72 ± 3.95	5.72 ± 2.92	4.734	< 0.001

pCR: pathological complete response.

ing a high degree of predictive accuracy for pCR in this patient cohort.

Discussion

This study evaluated the predictive potential of US features derived from elastography in assessing pCR in HER2-positive breast cancer patients undergoing NAT.

The relationship between posterior shadowing and pCR was particularly significant, with our results consistently showing a higher incidence of posterior shadowing in patients who

achieved pCR. This may be attributed to anatomical and physiological changes within the tumor during therapy. Posterior shadowing typically reflects greater tissue stiffness or density, characteristics often associated with malignancy. As tumors respond to NAT, cellular and structural changes can enhance posterior shadowing. Specifically, effective chemotherapy can induce fibrosis or necrosis, altering tissue acoustic properties and increasing shadowing.

The association observed in this study supports the hypothesis that changes in tissue architecture and density, as reflected by US features, may serve as surrogate markers of tumor responsiveness [18-20].

Strain ratio and strain difference were quantitative elastography metrics that reflect tissue stiffness. In our study, lower strain ratios and strain differences at week 6 were strongly correlated with pCR. These findings are consistent with the pathological process observed during effective NAT. As treatment progresses, responsive tumors typically undergo cellular lysis,

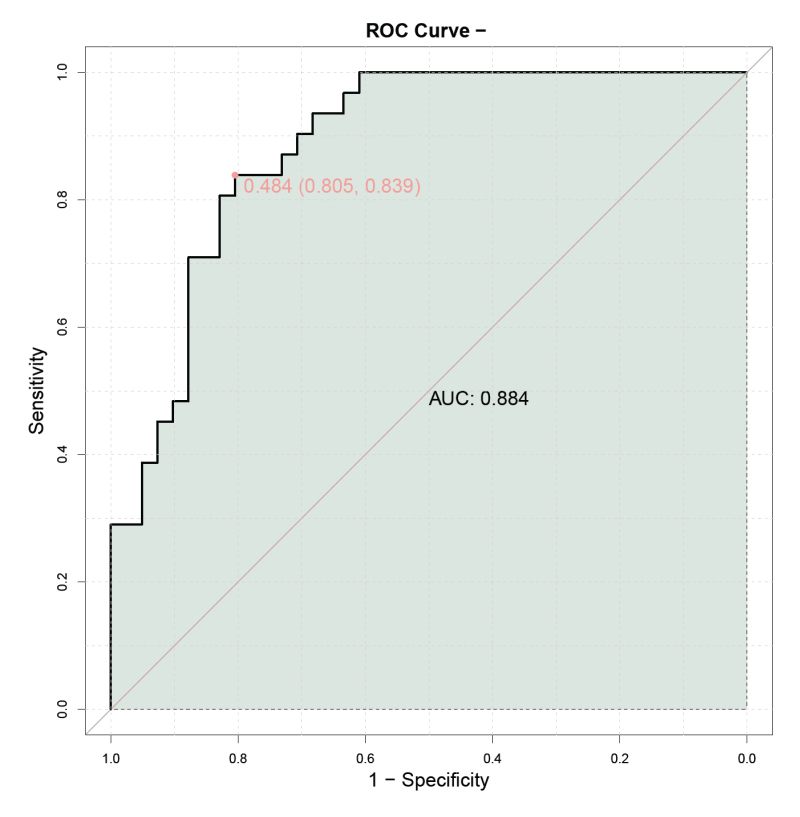


Figure 4. Combined predictive value of ultrasound features based on elastography for predicting pCR in HER2-positive breast cancer patients undergoing NAT (external validation). ROC: receiver operating characteristic; AUC: area under the curve; HER2: human epidermal growth factor receptor 2; pCR: pathological complete response; NAT: neoadjuvant therapy.

extracellular matrix remodeling, and necrosis, resulting in reduced tissue stiffness. Such biomechanical changes likely lead to lower strain ratio and difference values, reflecting effective tumor regression. The significant change in elastography metrics observed in the pCR group suggests that these measurements may effectively capture early treatment-induced mechanical changes within the tumor microenvironment, prior to detectable anatomical alterations by traditional imaging methods [21-23].

While these findings are promising, the precise biological mechanisms underlying changes in elastographic properties during NAT warrant further investigation. The observed reduction in stiffness may involve complex interactions among various cellular components, including the activation of apoptotic pathways and subsequent extracellular matrix degradation. Furthermore, variations in these metrics across study participants may reflect differenc-

es in individual tumor biology, such as cellular density, stromal composition, and vascularization, underscoring the need for personalized assessments [24, 25].

The study design, which included both internal and external validation cohorts, strengthens the generalizability of our findings. Consistent results across independent patient groups confirm the robustness of US elastographic features as predictors of pCR, underscoring their applicability in diverse clinical settings. However, potential operator dependency in elastography, as well as variations in equipment and settings across institutions, remain challenges. Efforts to standardize examination techniques and develop automated analysis protocols could mitigate these issues, enhancing reproducibility [26-28].

Integrating these elastographic metrics into clinical practice

requires careful consideration of cut-off values and diagnostic thresholds that optimize sensitivity and specificity [29, 30]. Our ROC analyses indicate high predictive accuracy, suggesting that combined metrics could serve as effective non-invasive assessment tools. However, practical implementation in clinical settings would necessitate validation through prospective studies to establish reliable benchmarks for predicting pCR, with sufficient accuracy to influence treatment decisions.

Another notable aspect is the potential costeffectiveness and accessibility of US elastography compared to more resource-intensive imaging modalities such as magnetic resonance imaging or positron emission tomography. Its non-invasive nature and real-time assessment capabilities offer advantages in both patient comfort and procedural efficiency. Incorporating elastography as a routine assessment tool in NAT settings could provide valuable insights earlier in the treatment course, enabling timely therapeutic adjustments and potentially improving patient outcomes [22, 31-33].

In combination with clinical and conventional imaging markers, elastographic features could significantly enhance predictive models of pCR. The high AUC values achieved through the integration of posterior features and strain metrics highlight the potential for comprehensive assessments that incorporate multiple data sources. Such multivariate models are crucial for capturing complex tumor dynamics and guiding personalized treatment strategies [34, 35].

While our study provides valuable insights into the predictive potential of US elastography features for pCR in HER2-positive breast cancer patients undergoing NAT, it has several limitations. First, the retrospective design of the study may introduce selection bias, and the use of de-identified patient data limits the ability to control for all potential confounding factors. Additionally, variations in the technical execution and interpretation of elastography across different operators and equipment could affect the reproducibility of results. Moreover, although the study was supported by external validation, the sample size may not be large enough to capture all possible variances in tumor biology and therapeutic response. Further prospective studies with standardized protocols are needed to confirm our findings and establish practical clinical thresholds for elastography metrics in predicting treatment outcomes.

Conclusion

Overall, our study enhances the understanding of US elastography's role in assessing treatment response in HER2-positive breast cancer patients. The findings could pave the way for more nuanced diagnostic frameworks that utilize the rich elasticity data provided by advanced imaging technologies. By improving our ability to predict pCR, clinicians can make informed decisions, potentially increasing the efficacy of NAT and ultimately improving patient prognosis in this cohort. Moving forward, continued efforts to optimize elastography protocols and

integrate them with molecular data are essential to fully realizing the potential of this promising diagnostic tool in oncologic care.

Disclosure of conflict of interest

None.

Address correspondence to: Yiru Cheng and Jianli Xue, Department of Ultrasound, The Fourth Hospital of Shijiazhuang, No. 16 Tangu North Street, Chang'an District, Shijiazhuang 050000, Hebei, China. E-mail: cyr20152357@163.com (YRC); xjl15233607900@163.com (JLX)

References

- [1] Katsura C, Ogunmwonyi I, Kankam HK and Saha S. Breast cancer: presentation, investigation and management. Br J Hosp Med (Lond) 2022; 83: 1-7.
- [2] Barzaman K, Karami J, Zarei Z, Hosseinzadeh A, Kazemi MH, Moradi-Kalbolandi S, Safari E and Farahmand L. Breast cancer: biology, biomarkers, and treatments. Int Immunopharmacol 2020; 84: 106535.
- [3] Wang H and Mao X. Evaluation of the efficacy of neoadjuvant chemotherapy for breast cancer. Drug Des Devel Ther 2020; 14: 2423-2433.
- [4] Shien T and Iwata H. Adjuvant and neoadjuvant therapy for breast cancer. Jpn J Clin Oncol 2020; 50: 225-229.
- [5] Huang JX, Shi J, Ding SS, Zhang HL, Wang XY, Lin SY, Xu YF, Wei MJ, Liu LZ and Pei XQ. Deep learning model based on dual-modal ultrasound and molecular data for predicting response to neoadjuvant chemotherapy in breast cancer. Acad Radiol 2023; 30 Suppl 2: S50-S61.
- [6] Bulut IN, Kayadibi Y, Deger E, Kurt SA, Velidedeoglu M, Onur I, Ozturk T and Adaletli I. Preoperative role of superb microvascular imaging and shear-wave elastography for prediction of axillary lymph node metastasis in patients with breast cancer. Ultrasound Q 2024; 40: 111-118
- [7] Wang Y, Li Y, Song Y, Chen C, Wang Z, Li L, Liu M, Liu G, Xu Y, Zhou Y, Sun Q and Shen S. Comparison of ultrasound and mammography for early diagnosis of breast cancer among Chinese women with suspected breast lesions: a prospective trial. Thorac Cancer 2022; 13: 3145-3151.
- [8] Jabeen K, Khan MA, Alhaisoni M, Tariq U, Zhang YD, Hamza A, Mickus A and Damaševičius R. Breast cancer classification from ultrasound images using probability-based opti-

- mal deep learning feature fusion. Sensors (Basel) 2022; 22: 807.
- [9] Catalano O, Fusco R, Carriero S, Tamburrini S and Granata V. Ultrasound findings after breast cancer radiation therapy: cutaneous, pleural, pulmonary, and cardiac changes. Korean J Radiol 2024; 25: 982-991.
- [10] Lee SC, Tchelepi H, Khadem N, Desai B, Yamashita M and Hovanessian-Larsen L. Imaging of benign and malignant breast lesions using contrast-enhanced ultrasound: a pictorial essay. Ultrasound Q 2022; 38: 2-12.
- [11] Gong H, Qian M, Pan G and Hu B. Ultrasound image texture feature learning-based breast cancer benign and malignant classification. Comput Math Methods Med 2021; 2021: 6261032.
- [12] Lee NR, Oh HK and Jeong YJ. Clinical significance of ultrasound elastography and fibrotic focus and their association in breast cancer. J Clin Med 2022; 11: 7435.
- [13] Kim SY, Lee HB, Han W, Lee SH, Chang JM and Cho N. Role of Doppler US and elastography prior to biopsy to identify candidates for avoidance of surgery following neoadjuvant chemotherapy for breast cancer. Ultrasonography 2023; 42: 323-332.
- [14] Cserni G. Histological type and typing of breast carcinomas and the WHO classification changes over time. Pathologica 2020; 112: 25-41.
- [15] Wahl RL, Jacene H, Kasamon Y and Lodge MA. From RECIST to PERCIST: evolving considerations for PET response criteria in solid tumors. J Nucl Med 2009; 50 Suppl 1: 122S-150S.
- [16] Saleh GA, Batouty NM, Gamal A, Elnakib A, Hamdy O, Sharafeldeen A, Mahmoud A, Ghazal M, Yousaf J, Alhalabi M, AbouEleneen A, Tolba AE, Elmougy S, Contractor S and El-Baz A. Impact of imaging biomarkers and ai on breast cancer management: a brief review. Cancers (Basel) 2023; 15: 5216.
- [17] Gouda MA, Janku F, Wahida A, Buschhorn L, Schneeweiss A, Abdel Karim N, De Miguel Perez D, Del Re M, Russo A, Curigliano G, Rolfo C and Subbiah V. Liquid biopsy response evaluation criteria in solid tumors (LB-RECIST). Ann Oncol 2024; 35: 267-275.
- [18] Luo H, Li J, Shi Y, Xiao X, Wang Y, Wei Z and Xu J. Stiffness in breast masses with posterior acoustic shadowing: significance of ultrasound real time shear wave elastography. BMC Med Imaging 2022; 22: 71.
- [19] Liu W, Li W, Li Z, Shi L, Zhao P, Guo Z, Tian J and Wang Z. Ultrasound characteristics of sclerosing adenosis mimicking breast carcinoma. Breast Cancer Res Treat 2020; 181: 127-134.

- [20] Bisquera OC Jr, Valparaiso AP, Espiritu NT, Ayuste EC Jr and Paloyo SR. Diagnostic validity of point-of-care breast ultrasound for females with palpable breast masses. Clin Breast Cancer 2023; 23: e189-e193.
- [21] Pan HY, Zhang Q, Wu WJ and Li X. Preoperative neoadjuvant chemotherapy in patients with breast cancer evaluated using strain ultrasonic elastography. World J Clin Cases 2022; 10: 7293-7301.
- [22] Jia W, Luo T, Dong Y, Zhang X, Zhan W and Zhou J. Breast elasticity imaging techniques: comparison of strain elastography and shearwave elastography in the same population. Ultrasound Med Biol 2021; 47: 104-113.
- [23] Hao Y, Ren G, Yang W, Zheng W, Wu Y, Li W, Li X, Li Y and Guo X. Combination diagnosis with elastography strain ratio and molecular markers effectively improves the diagnosis rate of small breast cancer and lymph node metastasis. Quant Imaging Med Surg 2020; 10: 678-691.
- [24] Zheng E, Zhang H, Goswami S, Kabir IE, Doyley MM and Xia J. Second-generation dual scan mammoscope with photoacoustic, ultrasound, and elastographic imaging capabilities. Front Oncol 2021; 11: 779071.
- [25] Ahn DY, Park HJ, Kim JN, Kim MS and Kang CH. Ultrasonographic and strain elastographic features of epidermal cyst according to body location. Acta Radiol 2023; 64: 1533-1539.
- [26] Zhou J, Zhang Q, Zhang Q, Yan L and Gao Q. Evaluation of the property of axillary lymph nodes and analysis of lymph node metastasis factors in breast cancer by ultrasound elastography. Comput Math Methods Med 2022; 2022: 8066289.
- [27] Zheng D, Li S, Ding Y, Chen H, Wang D, Wang H, Xie Y, Li C and Luo J. Effects of nurse-led hierarchical management care on acute stroke patients: a pilot study to promote stroke-associated pneumonia management. Front Neurol 2023; 14: 1121836.
- [28] Hoffmann R, Reich C and Skerl K. Evaluating different combination methods to analyse ultrasound and shear wave elastography images automatically through discriminative convolutional neural network in breast cancer imaging. Int J Comput Assist Radiol Surg 2022; 17: 2231-2237.
- [29] Sheng C, Gao S, Yan L, Yin H, Hu J, Ye Z and Wei X. Application value of conventional ultrasound combined with shear wave elastography in diagnosing triple negative breast cancer. Gland Surg 2021; 10: 1980-1988.
- [30] Cantisani V, David E, Barr RG, Radzina M, de Soccio V, Elia D, De Felice C, Pediconi F, Gigli S, Occhiato R, Messineo D, Fresilli D, Ballesio L and D'Ambrosio F. US-elastography for breast

Elastography predicts pathological response in HER2-positive breast cancer

- lesion characterization: prospective comparison of US BIRADS, strain elastography and shear wave elastography. Ultraschall Med 2021; 42: 533-540.
- [31] Park SY and Kang BJ. Combination of shear-wave elastography with ultrasonography for detection of breast cancer and reduction of unnecessary biopsies: a systematic review and meta-analysis. Ultrasonography 2021; 40: 318-332.
- [32] Jiang M, Li CL, Chen RX, Tang SC, Lv WZ, Luo XM, Chuan ZR, Jin CY, Liao JT, Cui XW and Dietrich CF. Management of breast lesions seen on US images: dual-model radiomics including shear-wave elastography may match performance of expert radiologists. Eur J Radiol 2021; 141: 109781.
- [33] Gu Y, Tian J, Ran H, Ren W, Chang C, Yuan J, Kang C, Deng Y, Wang H, Luo B, Guo S, Zhou Q, Xue E, Zhan W, Zhou Q, Li J, Zhou P, Zhang C, Chen M, Gu Y, Xu J, Chen W, Zhang Y, Li J, Wang H and Jiang Y. Can ultrasound elastography help better manage mammographic BI-RADS category 4 breast lesions? Clin Breast Cancer 2022; 22: e407-e416.

- [34] Xie L, Liu Z, Pei C, Liu X, Cui YY, He NA and Hu L. Convolutional neural network based on automatic segmentation of peritumoral shearwave elastography images for predicting breast cancer. Front Oncol 2023; 13: 1099650.
- [35] Li B, Zhao X, Wang Q, Jing H, Shao H, Zhang L and Cheng W. Prediction of high nodal burden in invasive breast cancer by quantitative shear wave elastography. Quant Imaging Med Surg 2022; 12: 1336-1347.